An Extension Gaussian Mixture Model for Brain MRI Segmentation

Yantao Song, Zexuan Ji, *Member*, *IEEE*, and Quansen Sun*, *Member*, *IEEE*

***Abstract*— The segmentation of brain magnetic resonance (MR) images into gray matter (GM), white matter (WM) and cerebrospinal fluid (CSF) has been an intensive studied area in the medical image analysis community. The Gaussian mixture model (GMM) is one of the most commonly used model to represent the intensity of different tissue types. However, as a histogram-based model, the spatial relationship between pixels is discarded in the GMM, making it sensitive to noise. Herein we present a new framework which aims to incorporate spatial information into the standard GMM, where each pixel is assigned its individual prior by leveraging its neighborhood information. Expectation maximization (EM) is modified to estimate the parameters of the proposed method. The method is validated on both synthetic and real brain MR images, showing its effectiveness in the segmentation task.**

I. INTRODUCTION

Brain disease has become one of the major threats of human health in recent years, and it becomes critically important to properly utilize medical examination and quantitative analysis for the diagnosis of brain diseases. A variety of brain imaging technology has been developed, where Magnetic resonance (MR) imaging has been widely used due to its better contrast for various brain tissues [1][2]. Many studies based on MRI scans, such as the quantitative analysis of tissue volumes, disease and injury diagnosis and surgical planning, requires segmentation of the imaged brain volume into three tissue types: gray matter (GM), white matter (WM) and cerebrospinal fluid (CSF). Consequently, segmentation methods of brain MR images into GM, WM and CSF has been an intensely studied research area.

In the last two decades, various approaches for brain MR segmentation have been developed [3][4][5][6], among which the GMM-based methods attract extensive attention. GMM is a useful probabilistic model for describing the image intensities of the different tissue classes, as the brain tissue intensity distribution can be well approximately by a Gaussian distribution and the contrast is high between different tissue classes. Furthermore, as a well-understood model [7], the GMM is computationally easy to implement using the EM algorithm, and therefore it has been widely used in the segmentation of brain MR images [4][8][9][10][11]. However, as an image histogram-based model, the spatial correlation between adjacent pixels is discarded in the GMM, making it very sensitive to noise. In order to overcome this limitation, many approaches have been proposed to incorporate spatial information into the segmentation to give spatially consistent results that are robust to noise. In particular, mixture models combined with Markov random field (MRF) has received great attention in the literature [10][12][13][14][15], as spatial correlation could be effectively captured through the MRF in a parametric way [16]. However, those models are computational expensive and it is not straightforward how to choose the underlying parameters for the optimal performance.

In this paper we propose a model based on standard GMM that incorporates the spatial correlation between neighborhood pixels with a simple patch metric, where a modified EM algorithm is used to optimize the parameters. We validate the proposed method using both synthetic and real dataset, and it compares favorably with several existing method.

II. METHOD

A. Gaussian Mixture Model

Gaussian mixture model is a histogram probabilistic model, image histogram reflects the frequency appears in a certain gray value, can also be considered as an estimation of probability density. Given a grayscale image with N pixels, we assume it can be divided into K different regions, so it shows K peaks in the histogram. Thus, the image can be represented by these K statistical models. By estimating the parameters of the GMM we can solve image segmentation problem.

The conditional distribution of the observation x_i given the class label k is assumed to be a univariant Gaussian distribution with parameter $\theta_k = (\mu_k, \sigma_k)$,

$$p(x_i|\theta_k) = \frac{1}{\sqrt{2\pi}\sigma_k} \exp(-\frac{(x_i - \mu_k)^2}{2\sigma_k^2}) \tag{1}$$

where μ_k and σ_k are the mean and the variance the distribution, respectively.

In the standard GMM, a common prior distribution π for the class label y_i is assumed for all image pixels, i.e.,

$$p(y_i = k|\pi) = \pi_k \tag{2}$$

with

$$0 \leq \pi_k \leq 1 \quad and \quad \sum_{k=1}^{K} \pi_k = 1 \tag{3}$$

*This work was supported by National Natural Science Foundation of China (61273251) and China Postdoctoral Science Fundation under Grant (2013M531364)

Yantao Song and Zexuan Ji are with the School of Computer Science and Engineering, Nanjing University of Science and Technology, Nanjing 210094, China (e-mail: yantaosong@hotmail.com; jizexuan@hotmail.com)

Quansen Sun is with the School of Computer Science and Engineering, Nanjing University of Science and Technology, Nanjing 210094, China (corresponding author, phone: +8613611507508, e-mail: sunquansen@njust.edu.cn)

978-1-4244-7929-0/14/$26.00 ©2014 IEEE

The density function for each observation x_i is given by

$$p(x_i|\theta_k, \pi_k) = \sum_{k=1}^{K} p(x_i|y_i = k, \theta_k)\pi_k \tag{4}$$

We note again that the prior π_k here does not depend on the pixel location.

The log-likelihood of all observations for the whole image is given by

$$\begin{aligned} L_1(\Theta, P) &= \sum_{i=1}^{N} \log p(x_i|\Theta, P) \\ &= \sum_{i=1}^{N} \log(\sum_{k=1}^{K} p(x_i|y_i = k, \theta_k)\pi_k) \end{aligned} \tag{5}$$

where $\Theta = (\theta_1, \theta_2, \ldots, \theta_K)$ is the parameter of GMM and P is the set of pixel labels y_i. As can be seen from the log-likelihood function in (5), the pixel x_i considered to be an independent sample without taking into account of the spatial relationship, and the same weight π_k is assigned for every pixel belonging to the class k. Although the standard GMM has a very simply form, as the pixels in the image vary both in their locations and intensity values, thus these insufficiencies make the standard GMM sensitive to noise.

By maximizing L_1 with respect to μ_k and σ_k, we can obtain the optimal parameters and then have the segmentation results.

$$(\Theta^*, P^*) = arg \max x_{\Theta,P} L_1(\Theta, P) \tag{6}$$

One of the technique is EM algorithm [5][17][18], approximating the optimal parameters by maximizing the log-likelihood iteratively.

B. The Proposed Method

In our method we introduce a new model based on GMM, which incorporates the spatial information by assigning each pixel with different prior probabilities inferred from its neighboring patch. Comparing to the standard GMM, the prior distributions π_{ij} are different for each pixel dependent on their locations.

$$p(y_i = k|\pi) = \pi_{ik} \tag{7}$$

Obviously, the proposed method takes into account of both intensity and spatial attributes of the pixels in a plain criterion. Furthermore, the proposed method is easier to implement and requires fewer parameters than state-of-the-art MRF-based models.

Given a grayscale image, we define N_i as a neighboring patch centered at pixel i, such as a 3×3 window. The prior probability distribution is assigned by all the neighborhood pixels in the same patch according to their similarity. Thus, we assign high value wherein adjacent pixels are similar. Specifically, with respect to the ith patch, we define a prior similarity function that represents the weight of each patch of pixel i for each class k

$$\psi_{N_i k} = \exp(-\frac{\beta}{2|N_i|} \sum_{m \in N_i} (\frac{\pi_{mk} + z_{mk}}{\| x_i - x_m \|^2})) \tag{8}$$

where z_{mk} is the posterior probability, β is the penalty factor that controlling the similarity function. Note that, the function $\psi_{N_i k}$ only dependents on the value of prior and posterior probability, and the main advantage of $\psi_{N_i k}$ is that it is easy to implement and incorporate the spatial correlation amongst neighboring pixels in a simple but systematic way.

The prior distribution has different values for each pixel corresponding to each class k in the image, given by

$$\pi_{ik} = \frac{\psi_{N_i k}}{\sum_{j=1}^{K} \psi_{N_i j}} \tag{9}$$

The prior probability π_{ik} in (9) is computed subject to the constraints

$$0 \leq \pi_{ik} \leq 1 \quad and \quad \sum_{k=1}^{K} \pi_{ik} = 1 \tag{10}$$

The log-likelihood function is given by

$$L_2^{(t+1)}(\Theta, P) = \sum_{i=1}^{N} \log(\sum_{j=1}^{K} \pi_{ij}^{(t)} p(y_i|\Theta)) \tag{11}$$

Comparing the log-likelihood function of the standard GMM in (5) with the proposed method in (11), the difference is the prior distribution π. Where in the proposed method the prior π is different for each pixel.

The posterior probability is

$$z_{ik}^{(t)} = \frac{\pi_{ik}^{(t)} p(y_i|\theta_k)}{\sum_{j=1}^{K} \pi_{ij}^{(t)} p(y_i|\theta_j)} \tag{12}$$

In order to maximize the log-likelihood function given in (11), the well-known EM algorithm is applied. Setting the derivative of the function in (11) with respect to μ_k and σ_k at the $(t+1)$ iteration step to zero, so then, we have

$$\mu_k^{(t+1)} = \frac{\sum_{i=1}^{N} z_{ik}^{(t)} x_i}{\sum_{i=1}^{N} z_{ik}^{(t)}} \tag{13}$$

$$\sigma_k^{(t+1)} = \frac{\sum_{i=1}^{N} z_{ik}^{(t)} (x_i - \mu_k^{(t+1)})(x_i - \mu_k^{(t+1)})^T}{\sum_{i=1}^{N} z_{ik}^{(t)}} \tag{14}$$

We summarize the pipeline of the proposed method as follows:

1) Initialize the mixture model component parameters $\theta_k = (\mu_k, \sigma_k)$, $k = (1, \ldots, K)$ and the prior probability π_{ik} for each pixel of each class.

2) Do until the convergence criterion is satisfied.

E-step:

Calculate the posterior probability z_{ik} by using(12);

M-step:

Update the mixture model parameters μ_{ik} and σ_{ik} by using (13), (14);

Calculate the prior similarity function of each neighboring patch $\psi_{N_i k}$ by using (8);

Update the prior probability π_{ik} by using (9);

3) End.

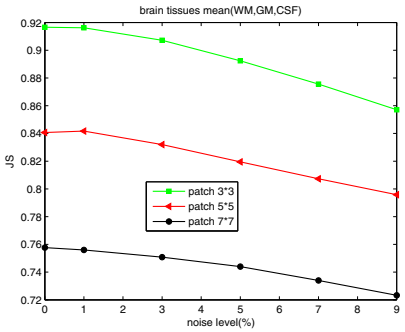

Fig. 1. JS with different patch size and different noise level for mean of brain tissues (WM,GM,CSF).

III. EXPERIMENTS AND DISCUSSIONS

In this section we demonstrate the performance of our algorithm on natural and brain images. The proposed method was compared to the standard GMM, GMM-based method [9] and the state-of-the-art MRF-based [17] method. In section 3-A, we discuss the choice of the neighboring patch size. Section 3-B presents segmentation results on both natural synthetic images and brain.

According to the characteristics of the image, we use different evaluation methods. For natural synthetic image, performance of the proposed method was compared with others by misclassification ratio (MCR) [13], which is the number of misclassified pixels divided by the total number of pixels. Two open datasets, BrainWeb and Internet brain segmentation repository (IBSR), are used as simulated and clinical test MR images respectively. To measure the accuracy ratio of the segmentation, we use the Jaccard Similarity (JS) coefficient [19] to calculate the overlap between segmentation results and ground-truth for each class. The JS score is defined as

$$JS(S_1, S_2) = \frac{|S_1 \cap S_2|}{|S_1 \cup S_2|}, \tag{15}$$

where S_1 and S_2 represent the segmentation volume and the standard ground-truth volume, respectively.

In all experiments, we use K-means algorithm as initialization, and the convergence criterion of the EM algorithm was defined as the percentage of change in the log-likelihood function. All methods were implemented and tested on a PC (Matlab R2010a, Core i5, running at 2.50GHz with 4GB of RAM).

A. Parameter Choice

In the first experiment, we discuss the impact of the size of neighboring patch. We applied our algorithm to 10 normal T1-weighted 3-D brain MR images selected from BrainWeb, in which the noise ranges from 0% to 90%. The variation of the JS for the mean of three tissues (WM, GM and CSF) with the noise level on different neighboring patch size is depicted in Fig.1.

As we can see from Fig.1, with the increase of noise and the patch size, the segmentation results get worse. This is because an overly-smoothed segmentation is attained when a big patch size used.

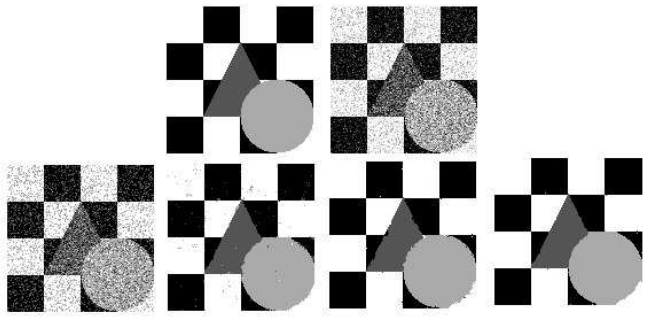

Fig. 2. Synthetic image (128×128, image resolution). First row, original image and corrupted original image with Gaussian noise (0 mean, 0.05 variance). Second row, from left to right, standard GMM method(MCR=54.88%), GMM-based method (MCR=3.26%), MRF-based method (MCR=1.45%), proposed method (MCR=0.96%).

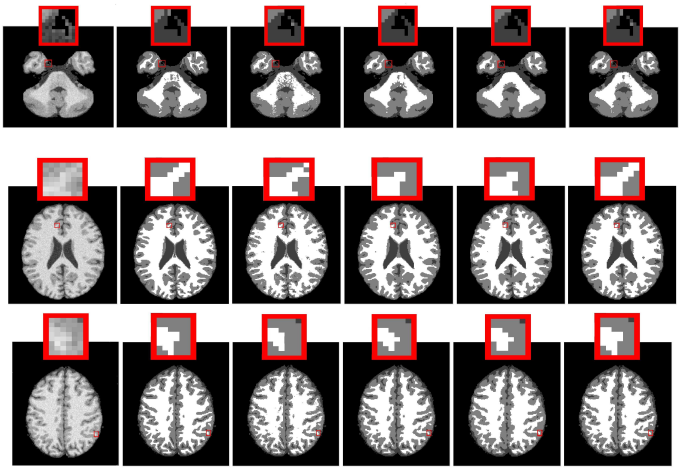

Fig. 3. Illustration of three slices extracted from a simulated T1-weighted ME study. From left to right: original image, ground truth, standard GMM method, GMM-based method, MRF-based method, proposed method.

The best results are attained using a 3×3 patch. In all our experiments, we used a 3×3 neighboring patch N_i for brain images, for natural images, we increase it to 5×5. The parameter β is empirically set to 10 in our experiments.

B. Image Experiments

1) Synthetic Image: In this section, a four-class synthetic image (128×128, shown in Fig.2) is used to compare the performance. The noisy image in Fig.2 is obtained by corrupting the original image with additive Gaussian noise (0 mean, 0.05 variance). As can be easily seen, the proposed

TABLE I
JS OF EACH SEGMENTATION ALGORITHM

method	WM	GM
standard GMM	0.6287	0.6888
GMM-based	0.8854	0.8501
MRF-based	0.8735	0.8635
proposed method	**0.9060**	**0.8919**

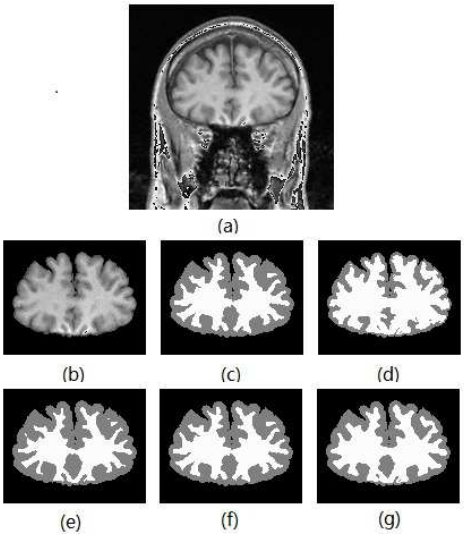

Fig. 4. Segmentation of a clinical MR image. (a) The original image. (b) The image of skull-stripping. (c) Ground truth. (d) The segmentation result of GMM method. (e) The segmentation result of GMM-based method. (f) The segmentation result of MRF-based method. (g) The segmentation result of proposed method

method outperforms other method with a lower MCR. The result demonstrates that our algorithm has a higher degree of robustness with respect to the high level of noise.

2) Brain Simulated Data: We evaluate the aforementioned segmentation algorithms on T1-weighted simulated brain MR image from BrainWeb dataset. The segmentation results obtained by applying these algorithms on MR image with 1mm cubic voxels and 5% noise, were shown in Fig.3. The result shows that the proposed method can preserve the details of the image. Although there are still some errors in our segmentation result, on the whole, the proposed method is superior than other methods, especially for small texture and complex topology.

3) Real Brain Data: For real brain MR image, we applied our algorithm to normal T1-weighted 3-D brain MR image selected from the IBSR. The resolution of the experimental image is $1\times1\times3$ mm, where the high resolution corresponds to coronal slices. Fig.4 shows the segmentation results of our algorithm with aforementioned algorithms and ground truth. The segmentation accuracy was measured by JS of GM and WM, and was compared in Table.1. It demonstrates again that our algorithm outperforms other methods in terms of segmentation accuracy.

IV. CONCLUSION

In this paper a novel extension of GMM for brain MR image segmentation is proposed, where correlation between neighboring pixels is incorporated into the standard GMM in a simple and systematic way. We validate our method on both simulated and real images. The result shows that our method compares favorably with several existing methods, producing accurate and robust segmentation results in presence of noise.

REFERENCES

[1] Toga A. and Mazziotta J., *Brain mapping: the methods. 2nd ed.*, San Diego: Academic press, 2002.

[2] Y. Ge, "The role of mr imaging," *AJNR Am J Neuroradiol*, vol. 27, pp. 1165–1176, 2006.

[3] A. W. Anderson C. Li, C. Xu and J. C. Gore, "Mri tissue classification and bias field estimation based on coherent local intensity clustering: A unified energy minimization framework," Information Processing in Medical Imaging, 2009, p. 288299.

[4] Quansen Sun Qiang Chen Deshen Xia Zexuan Ji, Yong Xia and David Dagan Feng, "Fuzzy local gaussian mixture model for brain mr image segmentation," *IEEE Transactions on Information Technology in Biomedicine*, vol. 16, pp. 339–347, 2012.

[5] D. Vandermeulen V. Leemput, K. Maes and P. Suetens, "Automated model-based bias field correction of mr images of the brain," *IEEE Transactions on Medical Imaging*, vol. 18, pp. 885–896, 1999.

[6] Quansen Sun Qiang Chen Deshen Xia Zexuan Ji, Yong Xia and David Dagan Feng, "Fuzzy c-means clustering with weighted image patch for image segmentation," *Applied Soft Computing*, vol. 12, pp. 1659–1667, 2012.

[7] Bishop C M., *Pattern Recognition and Machine Learning*, Berlin: Springer-Verlag, 2006.

[8] Vlassis N. Verbeek J. J. and Krose B., "Efficient greedy learning of gaussian mixture models," *Neural Computation*, vol. 15, pp. 469–485, 2003.

[9] Q.M.J. Wu M.N. Thanh and S. Ahuja, "An extension f the standard mixture model for image segmentation," *IEEE Transactions on Neural Networks*, vol. 21, pp. 1326–1338, 2010.

[10] Saripan M. I. Balarf M. A., Ramli A. R. and Mashohor S., "Review of brain mri image segmentation methods," *Artificial Intelligence Review*, vol. 33, pp. 261–274, 2010.

[11] M.N. Thanh and Q.M.J. Wu, "Fast and robust spatially constrained gaussian mixture model for image segmentation," *IEEE Transactions on Circuits and Systems for Video Technology*, vol. 23, pp. 621–635, 2013.

[12] B.J. Krause W. M. Wells K. Held, E. R. Kops and R. Kikinis, "Markov random field segmentation of brain mr images," *IEEE Transactions on Medical Imaging*, vol. 16, pp. 878–886, 1997.

[13] Brady M. Zhang Y. and Smith S., "Segmentation of brain mr images through a hidden markov random field model and the expectation maximization algorithm," *IEEE Transactions on Medical Imaging*, vol. 20, pp. 45–57, 2001.

[14] Geman S. and Geman D., "Stochastic relaxation, gibbs distributions, and the bayesian restoration of images," *IEEE Transactions on Pattern Analysis and Machine Intelligence*, vol. 6, pp. 721–741, 1984.

[15] Azmi Reza Yousefi Sahar and Zahedi Morteza, "Brain tissue segmentation in mr images based ona hybrid of mrf and social algorithms," *Medical Image Analysis*, vol. 16, pp. 840–848, 2012.

[16] Q.M.Jonathan Wu Hui Zhang and Thanh Minh Nguyen, "Image segmentation by a robust modified gaussian mixture model," in *ICASSP*. IEEE, 2013, pp. 1478–1482.

[17] Vlassis N. Diplaros A. and Gevers T., "A spatially constrained generative model and an em algorithm for image segmentation," *Neural Networks*, vol. 18, pp. 798–808, 2007.

[18] G. J. McLachlan and T. Krishnan, *The EM algorithm and extensions*, New York: Wiley, 1997.

[19] Pernug F. Vovk U. and Likar B., "A review of methods for correction of intensity inhomogeneity in mri," *IEEE Transactions on Medical Imaging*, vol. 26, pp. 405–421, 2007.